A phage mechanism for selective nicking of dUMP-containing DNA

Tridib Mahata[a], Shahar Molshanski-Mor[a], Moran G. Goren[a], Biswanath Jana[a], Miriam Kohen-Manor[a], Ido Yosef[a], Oren Avram[b], Tal Pupko[b], Dor Salomon[a,1], and Udi Qimron[a,1]

[a]Department of Clinical Microbiology and Immunology, Sackler School of Medicine, Tel Aviv University, 69978 Tel Aviv, Israel; and [b]The Shmunis School of Biomedicine and Cancer Research, George S. Wise Faculty of Life Sciences, Tel Aviv University, 69978 Tel Aviv, Israel

Edited by Charles C. Richardson, Harvard Medical School, Boston, MA, and approved April 29, 2021 (received for review December 22, 2020)

Bacteriophages (phages) have evolved efficient means to take over the machinery of the bacterial host. The molecular tools at their disposal may be applied to manipulate bacteria and to divert molecular pathways at will. Here, we describe a bacterial growth inhibitor, gene product T5.015, encoded by the T5 phage. High-throughput sequencing of genomic DNA of bacterial mutants, resistant to this inhibitor, revealed disruptive mutations in the *Escherichia coli ung* gene, suggesting that growth inhibition mediated by T5.015 depends on the uracil-excision activity of Ung. We validated that growth inhibition is abrogated in the absence of *ung* and confirmed physical binding of Ung by T5.015. In addition, biochemical assays with T5.015 and Ung indicated that T5.015 mediates endonucleolytic activity at abasic sites generated by the base-excision activity of Ung. Importantly, the growth inhibition resulting from the endonucleolytic activity is manifested by DNA replication and cell division arrest. We speculate that the phage uses this protein to selectively cause cleavage of the host DNA, which possesses more misincorporated uracils than that of the phage. This protein may also enhance phage utilization of the available resources in the infected cell, since halting replication saves nucleotides, and stopping cell division maintains both daughters of a dividing cell.

T5 bacteriophage | ung | endonuclease | toxic protein | AP site

Phages have coevolved with bacteria for eons and have consequently developed mechanisms to specifically and optimally inhibit or divert key host metabolic functions. Increasing the knowledge about the bacterial pathways targeted by phages and identifying the disruptive gene products used against them may generate tools to manipulate bacteria. It is therefore important to examine strategies for identifying these interactions.

In recent years, we and others identified several phage products that control bacterial metabolism. For example, we discovered a phage protein inhibiting the essential cell division protein FtsZ (1) and another inhibiting the essential cytoskeletal protein MreB (2). It is likely that there are many additional, yet unidentified, phage products that inhibit novel bacterial targets.

A model for the systematic study of host–virus interactions and examination of phage antibacterial strategies is provided by the phages and their host, *Escherichia coli*. The laboratory strain *E. coli* K-12 shares many essential genes with pathogenic strains, such as *E. coli* O157:H7 and O104:H4; therefore, growth inhibitors against K-12 should also prove effective against these pathogens. *E. coli* has been studied extensively, and the putative functions or tentative physiological roles of over half of its 4,453 genes have been identified.

T5 is an obligatory-lytic phage of *E. coli*, whose successful growth cycle results in lysis of the host. Specific functions have been attributed to many of the gene products (3); the phage structural gene products are well characterized, as are those gene products that take part in phage DNA replication. However, despite intensive study, the mechanism by which it manipulates host functions remains obscure. Since many of the pre-early and early genes have not yet been characterized, and the host proteins with which they interact have not been identified, we hypothesized that some of these gene products might be responsible for inhibiting *E. coli* growth by targeting specific host proteins or pathways.

We previously developed an approach designed to search for antibacterial targets of phage proteins by using whole-genome DNA-sequencing (DNA-seq) (2). The basic underlying principle is that mutations conferring resistance against growth inhibitors may arise in target genes. Therefore, we can identify the target by expressing a growth inhibitor and using DNA-seq to identify mutations responsible for resistance. Advances in DNA-seq technology, as well as improvements in accessibility and affordability, now enable the use of this procedure for the identification of bacterial targets at high throughput and low cost. Here, we describe the use of this technique to search for bacterial targets of phage proteins and the identification of an interaction between a T5 inhibitory phage protein and the *E. coli* Uracil DNA glycosylase (Ung).

Ung is an enzyme involved in DNA repair in all living organisms. It excises uracils misincorporated into the DNA as a result of erroneous use of the deoxyuridine 5′-triphosphate (dUTP) nucleotide by DNA polymerase or due to deamination of cytosine (4). Release of the uracil from the DNA results in a potentially cytotoxic abasic site (known as an apurinic/apyrimidinic site; henceforth referred to as an AP site) because it blocks DNA synthesis (5). AP endonuclease activities such as those associated with exonuclease III, endonuclease III, and endonuclease IV can then cleave the DNA at the resulting AP sites, resulting in a nicked DNA strand (6).

Significance

Studying the interactions of bacterial viruses (phages) with their bacterial hosts may lead to better understanding of bacterial mechanisms and consequently enable better manipulation of bacterial pathogens. In this study, we characterized the activity of a protein from phage T5, called T5.015. This protein binds to another protein, Ung, and uses its activity to selectively cleave dUMP-containing DNA. Such cleavage of the bacterial DNA stops bacterial DNA replication and also prevents bacterial division. Presumably, the phage DNA is protected from this activity as Ung does not act on the phage DNA, probably due to lower incorporation of the Ung substrate, dUMP. We believe that the findings are general to many phages and reveal a mechanism of self-versus-foreign DNA discrimination.

Author contributions: T.M., S.M.-M., M.G.G., I.Y., O.A., T.P., D.S., and U.Q. designed research; T.M., S.M.-M., M.G.G., B.J., and M.K.-M. performed research; T.M., S.M.-M., M.G.G., B.J., I.Y., O.A., T.P., D.S., and U.Q. analyzed data; and D.S. and U.Q. wrote the paper.

The authors declare no competing interest.

This article is a PNAS Direct Submission.

[1]To whom correspondence may be addressed. Email: dorsalomon@mail.tau.ac.il or ehudq@post.tau.ac.il.

This article contains supporting information online at https://www.pnas.org/lookup/suppl/doi:10.1073/pnas.2026354118/-/DCSupplemental.

Published May 31, 2021.

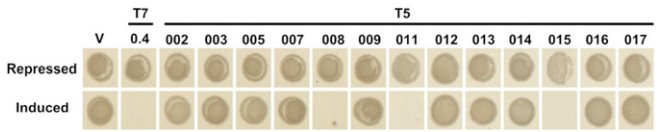

Fig. 1. Identification of T5 phage gene products inhibiting bacterial growth. *E. coli* NEB5-α bacteria transformed with a plasmid encoding the indicated phage T5 gene products were inoculated on LB agar plates supplemented with 0.2% D-glucose (Repressed) or 0.2% L-arabinose (Induced). Results of a representative experiment are shown. Empty vector (V) was used as a negative control; phage T7 gene 0.4, which is known to inhibit bacterial growth, was used as a positive control.

In this study, we show that a T5 phage protein, T5.015, physically interacts with Ung to inhibit bacterial growth. Remarkably, T5.015 exploits Ung to identify and localize to Ung-generated AP sites in the DNA, which it cleaves to form a nick. This unprecedented mechanism of action results in DNA replication and cell division arrest.

Results

T5 Phage Gene Products Inhibit *E. coli* Growth. To identify genes that inhibit bacterial growth, we cloned 13 pre-early and early genes of unknown function from phage T5, together with their natural ribosome binding sites, into plasmid pBAD33 under the tightly regulated pBAD promoter (7). These genes were as follows: T5.002, T5.003, T5.005, T5.007, T5.008, T5.009, T5.011, T5.012, T5.013, T5.014, T5.015, T5.016, and T5.017. *E. coli* NEB5-α cultures harboring individual plasmids for inducible expression of the aforementioned genes were inoculated on Luria-Bertani (LB) agar plates with or without the inducer, L-arabinose. Using this approach, we identified three genes, T5.008, T5.011, and T5.015 (henceforth called 008, 011, and 015, respectively) as toxic to the bacterial host (Fig. 1). In this study, we focused on gene 015.

Phylogeny of 015 Homologs. First, we set out to determine how widespread 015 homologs are. We found that 015 homologs are widely distributed among various members of the Markadamsvirinae subfamily of phages, including mainly phages that target the human pathogens *E. coli* and *Salmonella* as well as one phage that targets *Yersinia* (*SI Appendix*, Fig. S1). A few homologs are described as bacterial genes; however, inspection of their genetic neighborhoods suggests that they are possibly phage genes, which have been misannotated as part of the bacterial genome (e.g., EFG4537521.1).

Isolation of *E. coli* Mutants Resistant to 015. To identify the target of 015, we plated ~10^9 bacteria harboring the 015-encoding plasmid under inducing conditions and isolated resistant mutants. Such resistant mutants may arise from plasmid loss or from mutations in 015 that render it ineffective. Alternatively, they may arise from genomic mutations in a gene whose product is targeted by 015. To exclude plasmid loss or 015 mutants, we extracted the plasmids from resistant colonies and validated their toxicity by transforming them into naïve bacterial cells. In this way, we identified eight clones containing plasmids that retained toxicity, indicating that they harbor genomic mutations conferring resistance to 015. These clones were used in subsequent analyses.

Mutations in *ung* Eliminate 015-Mediated Toxicity. The genomic DNA of all eight mutants that were resistant to the expression of 015 was sequenced in an Illumina-based high-throughput sequencer. The results yielded ~30× coverage of each genome, which is sufficient to detect single-nucleotide polymorphisms (SNPs) with a high confidence score (2). An analysis of the deep DNA-seq revealed that the *ung* gene, encoding the enzyme responsible for removing uracil bases from DNA (4, 5), was specifically mutated in all the 015-resistant clones (*SI Appendix*, Table S1). The mutations were then confirmed using Sanger sequencing. Since Ung is not essential to bacterial growth (8), the mechanism of 015-mediated toxicity cannot be explained by inhibition of Ung activity. This suggests that the toxicity mediated by 015 results from its interaction with a functional Ung.

A Functional Ung Is Required for 015-Mediated Toxicity. To confirm that 015-mediated toxicity is dependent on the presence of a functional Ung, we first determined whether expression of 015 affects the growth of a Δ*ung* mutant. In agreement with the notion that 015 requires Ung to mediate its toxic effect, expression of 015 did not inhibit the growth of a Δ*ung* strain (Fig. 2*A*). The toxicity was restored upon expression of *ung* from a plasmid (pUng), indicating that the loss of toxicity was a direct result of absence of *ung* and not due to an offsite mutation or a polar effect resulting from the deletion. Phage T7 gene 0.4, which does not require *ung* to inhibit *E. coli* (1), was used as a control and indeed remained toxic after deletion of *ung*. To further support the dependence of 015 on a functional Ung, we evaluated the effect of Ugi, an inhibitor of Ung produced by phage PBS2, on 015-mediated toxicity. As predicted, expression of Ugi in ung^+ *E. coli* cells coexpressing 015, rescued bacteria from 015-mediated toxicity (Fig. 2*B*). Taking the above results together, we conclude that 015 requires a functional Ung to inhibit bacterial growth.

015 Specifically Interacts with Ung. Next, we determined whether 015 physically interacts with Ung. The results of a pull-down assay revealed that a 6× His-tagged Ung interacts with 015 tagged with calmodulin-binding peptide (CBP) but not with the phage T7 protein 1.4 that was used as a control (Fig. 3*A*). The interaction was direct, as it was reproduced with purified proteins (*SI Appendix*, Fig. S2*A*); it was also specific, as nonspecific binding of 015 to the resin was not observed (*SI Appendix*, Fig. S2*B*).

Additionally, coexpression of 015 and Ung fused to the fluorescent proteins sfGFP and mCherry, respectively, on a Δ*ung* *E. coli* background revealed their colocalization. While 015-sfGFP localized mostly to puncta at the cell poles in the absence of Ung, in the presence of Ung, it was redistributed and exhibited a diffusible pattern with several puncta, overlapping with Ung-mCherry. Notably, puncta showing colocalization of 015 and Ung also overlapped with Hoechst-stained DNA (Fig. 3*B*). Since the bacterial cells elongate and lack distinct poles in the presence of a functional 015, we repeated these experiments using a 015 mutant

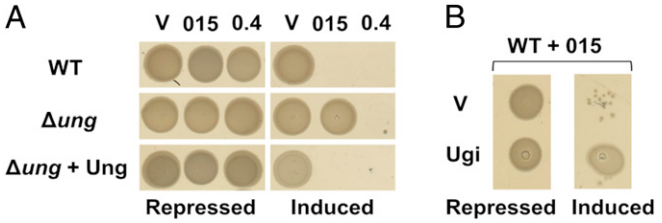

Fig. 2. 015-mediated toxicity depends on a functional Ung. (*A*) Growth of *E. coli* BW25113 bacteria, either wild type (WT), Δ*ung* (Δ*ung*), or Δ*ung*-harboring pUng for expression of Ung (Δ*ung* + Ung), transformed with a plasmid encoding a control vector (V), $p015^{kan}$ encoding T5 gene 015 (015), or the $p0.4^{kan}$ encoding T7 gene 0.4 (0.4) as a growth inhibitor positive control. Cultures were inoculated on LB agar supplemented with 0.2% D-glucose (Repressed) or 0.2% L-arabinose (Induced). (*B*) Growth of *E. coli* NEB5-α bacteria cotransformed with the plasmid $p015^{kan}$ encoding the T5 gene 015 (WT + 015) and either a control vector (V) or the pUgi vector expressing the Ung inhibitor, Ugi. Bacteria were inoculated on LB agar supplemented with 0.2% D-glucose (Repressed) or 0.2% L-arabinose and 1 mM IPTG (Induced). Experiments were performed at least twice. Results of a representative experiment are shown.

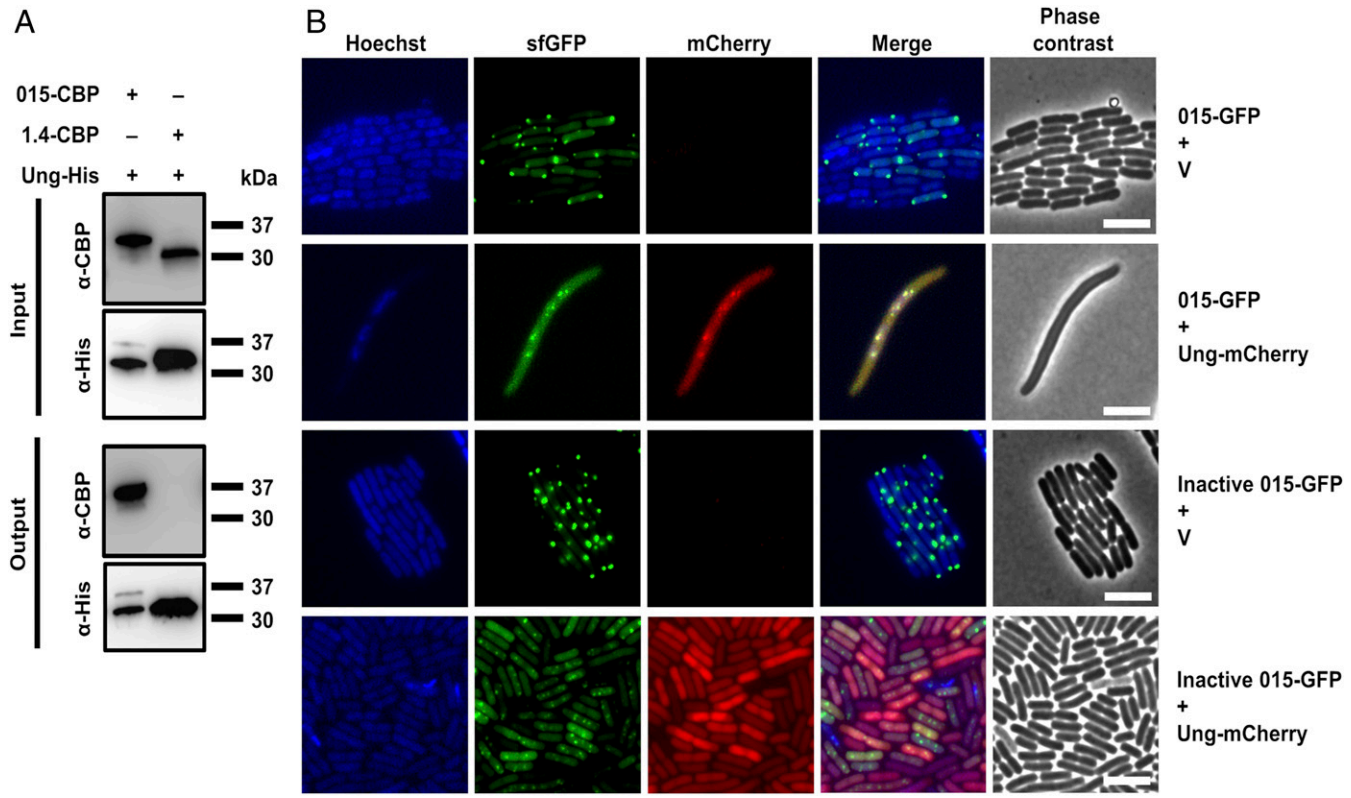

Fig. 3. Ung interacts with 015. (*A*) Ni-Agarose resin pull-down of plasmid-encoded His-tagged Ung expressed in *E. coli* BW25113 Δ*ung*-harboring CBP-tagged 015 or 1.4. Antibodies against the His tag or the CBP tag (α-His and α-CBP, respectively) were used for Western blot. (*B*) Sample images of *E. coli* BW25113 Δ*ung* cells containing the indicated combinations of arabinose-inducible plasmids expressing the wild-type 015 or the inactive $015^{K85A,K94A,K111A}$ mutant both fused to superfolder GFP (015-GFP and Inactive 015-GFP, respectively), with either an empty vector (V) or Ung fused to mCherry (Ung-mCherry). Bacteria were induced for 30 min with 0.01% L-arabinose, followed by staining with Hoechst 33342. (Scale bar, 5 μm.)

that does not cause cell elongation. Three substitutions of lysines in this mutant make it noninhibitory to cell growth while maintaining its binding capability to Ung (*SI Appendix*, Fig. S3). Experiments with this mutant showed similar results (Fig. 3*B*). These results suggest that 015 interacts with Ung inside the cell and that the two proteins colocalize and concentrate at distinct DNA-containing regions.

015 Induces Cell Elongation and DNA Condensation. Interestingly, coexpression of 015 and Ung resulted in dramatic cell elongation and the formation of nucleoid structures (Fig. 3*B*). To further investigate the nature of these phenotypes, we monitored *ung*$^+$ *E. coli* cells expressing 015 from a plasmid over time. As shown in *SI Appendix*, Fig. S4, cells expressing 015 increased in length over time and exhibited condensed DNA, suggesting a defect in cell division.

015 Induces DNA Replication Arrest. The observed phenotypes, including cell elongation and DNA condensation (Fig. 3 and *SI Appendix*, Fig. S4), are often the consequence of DNA replication arrest (9). To determine whether 015 affects DNA replication, we used real-time PCR to monitor the ratio of the origin of replication (*oriC*) to the terminus of the *E. coli* chromosome (*ter*) as an indicator of chromosome replication. In cells in which DNA replication is uninterrupted, the ratio should be close to 1, whereas replication arrest will cause the ratio to increase as a lower number of replication forks are able to reach the terminus. As expected, treating *E. coli* cells with trimethoprim, an inhibitor of DNA synthesis (10), resulted in an approximately twofold increase in the *oriC*/*ter* ratio compared to untreated cells (Fig. 4*A*). Interestingly, expression of 015 resulted in an approximately sixfold increase in the *oriC*/*ter* ratio, indicating that in the presence of 015, chromosomal replication is not completed and replication forks do not reach the terminus.

The efficiency of chromosomal replication was estimated by using MiSeq to analyze the depth of coverage. Notably, we observed a peak in replication at, and adjacent to, the chromosomal *oriC* in cells expressing 015, whereas control cells containing an empty expression vector exhibited a uniform level of replication throughout the chromosome (Fig. 4*B*). Taken together, these results demonstrate that 015 induces DNA replication arrest in the host cell, leading to cell elongation and DNA condensation. Furthermore, the observed continued cell elongation suggests that there is no inhibition of protein synthesis by 015.

015 Uses Ung to Cleave AP Sites. Our findings that 015 binds Ung and induces DNA replication arrest prompted us to hypothesize that 015 exploits Ung to modify the host DNA and thereby inhibit host growth. Since Ung recognizes uracil incorporated into the DNA and cleaves the *N*-glycosidic bond to generate an AP site (4), we set out to determine whether these Ung-generated AP sites are targeted by 015. To this end, we devised an assay to monitor the effect of treatment with Ung and 015 on the integrity of a DNA strand containing a uracil. We constructed a 28-bp double-stranded DNA (dsDNA) oligomer in which one strand is labeled with a Cy5.5 fluorophore at the 5′ end and contains a uracil at position 14 (Fig. 5*A*). Incubation of this dsDNA oligomer with Ung produces an AP site at the position occupied by the uracil. Although this modification alone does not affect the integrity of the DNA strand backbone, a subsequent cleavage event at the newly made AP site will nick the DNA strand backbone, resulting in a shorter Cy5.5-labeled strand (Fig. 5*A*). Cleaved and uncleaved Cy5.5-labeled

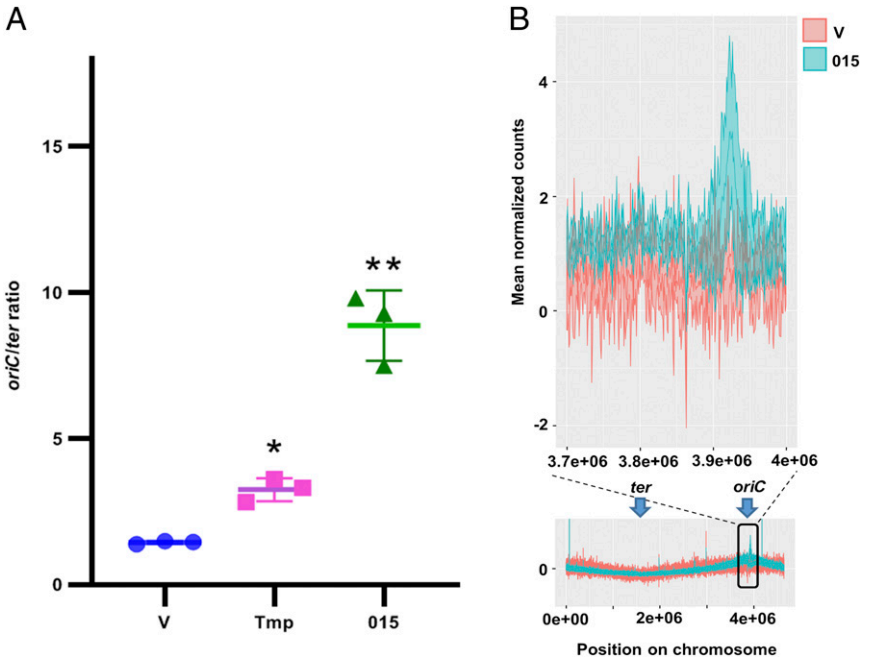

Fig. 4. 015 activity results in DNA replication arrest. (*A*) *oriC* to *ter* ratio as determined by real-time PCR performed on DNA extracted from *E. coli* MG1655 cells containing a control expression vector (V), treated or untreated with Trimethoprim (Tmp), or containing plasmid p015^{kan} for arabinose-inducible expression of 015 (015). Data represent the mean ± SD ($n = 3$). Asterisks denote statistical significance compared to control vector (V) sample by unpaired, two-tailed Student's *t* test (*$P = 0.0178$, **$P = 0.0079$). (*B*) Coverage analysis across the genome of *E. coli* MG1655 harboring arabinose-inducible pBAD33^{kan} plasmids, either control (V) or p015^{kan} encoding 015 (015). A magnification of the readings in the *oriC* vicinity is shown in the top. The *y*-axis shows the *z*-score of the counts; the *x*-axis denotes the position on the genome. *oriC* and ter are marked by blue arrows.

strands can then be distinguished by resolving the treated DNA on a denaturing urea polyacrylamide gel to separate the dsDNA into single-stranded DNA, followed by visualization of Cy5.5 fluorescence.

As expected, treatment of the dsDNA oligomer with Ung alone did not produce cleavage of the DNA backbone (Fig. 5*B*). However, when we incubated the dsDNA with Ung together with apurinic/apyrimidinic endonuclease (Ape1), an enzyme that recognizes and cleaves AP sites (6), a lower band corresponding to a cleaved DNA product appeared on the gel. Remarkably, a similar lower band appeared when the dsDNA oligomer was treated with Ung and purified His-tagged 015 (Fig. 5*B* and *SI Appendix*, Fig. S5), suggesting that 015 can also cleave the DNA backbone at the AP site generated by Ung. The specific activity of the purified 015 was low, probably due to a high percentage of misfolded protein; therefore, throughout the experiments, an excess of 015 over the substrate was used. The activity was further tested with lower 015 concentrations, showing complete nicking of the substrate incubated with 851 nM of purified 015 protein for 6 h (*SI Appendix*, Fig. S6). We noted that in contrast to cleavage by Ape1, the efficiency

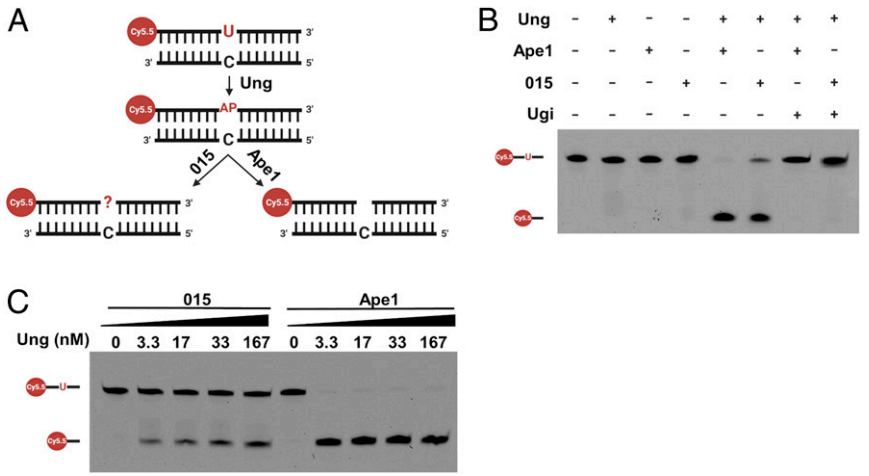

Fig. 5. 015 cleaves Ung-generated AP sites. (*A*) Schematic diagram of the Ung-generated AP site cleavage assay. (*B* and *C*) AP site cleavage assay performed in the presence of the Cy5.5-labeled dsDNA oligomer and the indicated purified proteins. In *B*, 33.4 nM (1 U) of Ung, 6.6 nM (2 U) of Ape1, 1.26 μM of 015, and 820 nM (2 U) of Ugi were used. In *C*, 315 nM of 015 and 6.6 nM of Ape1 were used. Cy5.5 fluorescence of assay products resolved on denaturing urea polyacrylamide gel are shown.

of 015-mediated cleavage of the AP site correlated with increasing Ung concentration (Fig. 5*C*). One possible explanation for the observed partial cleavage is that 015 inhibits Ung. However, the addition of Ape1 to the reaction showed complete nicking, regardless of the presence of 015, indicating that Ung is not inhibited by 015 and fully generates the AP sites even in the presence of 015 (*SI Appendix*, Fig. S7). These results, taken together with the ability of 015 to bind to and colocalize in vivo with Ung, suggest that 015 acts together with Ung to cleave the AP sites.

015 Directly Catalyzes Nicking of Ung-Generated AP Sites. Next, we set out to determine which subunit of the 015-Ung heterocomplex catalyzes cleavage of the AP site. To this end, we examined whether we could separate the activities of Ung and 015 by treating dsDNA oligomers with Ung to generate an AP site, followed by the removal of Ung by phenol–chloroform extraction. The AP site–containing dsDNA oligomers were then incubated with purified His-tagged 015. As shown in Fig. 6*A*, 015 was able to cleave the Ung-generated AP site in vitro, even in the absence of Ung in a similar fashion to the Ape1 control. However, 015 was unable to cleave dsDNA oligomers that had not been pretreated with Ung and therefore lacked an AP site. This result suggests that 015, rather than Ung, catalyzes the cleavage of the AP site.

Finally, we determined the apparent chemical nature of the nick formed by 015. We compared the mobility of the product of 015 to the mobility of products obtained by other enzymes: 1) Formamidopyrimidine DNA Glycosylase (Fpg), an AP-lyase producing a nick with a δ elimination termini (Fig. 6*B*); 2) endonuclease III (Endo-III), an AP endonuclease producing a nick with a β-elimination termini (Fig. 6*B*); and 3) Ape1, an AP endonuclease producing a nick with a hydrolytic cleavage termini. Incubation of an AP DNA substrate with each of the above enzymes, followed by gel electrophoresis, revealed that 015 produces a product identical in its electrophoretic mobility to that produced by Ape1 in both the 3′ and 5′ ends. These results suggests that a 3′-OH and a 5′-deoxyribose 5-phosphate (5′-dRP) termini are produced by 015 cleavage (Fig. 6 *C* and *D*). Taken together, our results demonstrate that 015 utilizes an unprecedented mechanism to damage the host cell by exploiting Ung to localize to AP sites on the bacterial chromosome and mediating DNA cleavage, leading to DNA replication and cell division arrest.

Discussion

In this work, we employed a genetic approach comprising high-throughput DNA-seq of resistant bacterial mutants to identify the target of 015, a phage T5 gene product that inhibits bacterial growth. We showed that 015 binds Ung to localize to Ung-generated AP sites and cleave them, leading to DNA replication arrest. The mechanism employed by 015 to damage the bacterial host cell is unprecedented; while previously described phage-borne toxins directly inhibit or target an essential bacterial component, 015 exploits a nonessential host protein to target specific sites on the host DNA (Fig. 7).

Here, we report a phage protein that utilizes a nonessential host protein for nicking the host DNA strands. Related toxicity mechanisms have been reported for bacterial toxins that inhibit target bacteria by using their proteins for cleaving transfer RNAs (tRNAs) (11–13). One recent example is that of the contact-dependent tRNAse CdiA-CT^{EC869} toxin encoded by *E. coli* EC869 (13). This toxin, transferred from the inhibitor bacteria to the target bacteria, binds to elongation factors of the target bacteria. The binding to the host factors is critical for the tRNase toxic activity, similar to the dependence of 015 toxicity on Ung.

Specifically targeting Ung-generated AP sites equips the phage with a mechanism to discriminate between the host and phage genomes. The phage also encodes a potent deoxyuridine 5′-triphosphate nucleotidohydrolase (dUTPase), an enzyme that substantially reduces the cell's UTP levels upon infection (14). This ensures that uracils are not incorporated into newly replicated phage genomes so that when a phage infects a new bacterium, its DNA is devoid of uracils that can be identified and modified by Ung into 015-targetable AP sites. Conversely, the host DNA has been seeded with uracils prior to the infection, and these are targeted by Ung to generate 015 target sites. Arresting only the replication of the host chromosome by this mechanism provides a means to hijack the cellular resources to

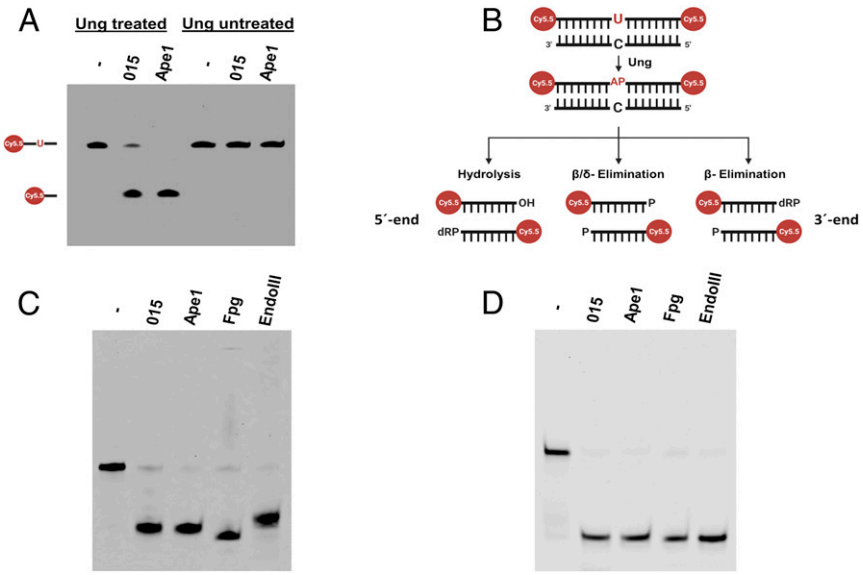

Fig. 6. 015 catalyzes the cleavage of AP sites. (*A*) AP site cleavage assay performed on Ung pretreated or untreated dsDNA oligomers. Ung was removed from treated DNA followed by addition of purified 015 (1.26 μM), Ape1 (6.6 nM), or buffer (–). (*B*) Schematic representation of the 3′ (*Top*) and 5′ (*Bottom*) termini produced by hydrolysis (Ape1), β elimination (Fpg), and β\δ elimination (Endonuclease III). To determine the electrophoretic mobility of the 015-generated 3′-terminus (*C*) or the 5′-terminus (*D*), compared to termini generated by the above-mentioned enzymes, substrate DNA with either 5′-Cy5.5 or 3′-Cy5.5, respectively, was incubated with UNG (33.4 nM) together with either 015 (946 nM), Ape1 (33 nM), Fpg (1.28 μM), or Endonuclease III (89.1 nM). Cleaved products with 3′ termini and 5′ termini were separated on urea-PAGE.

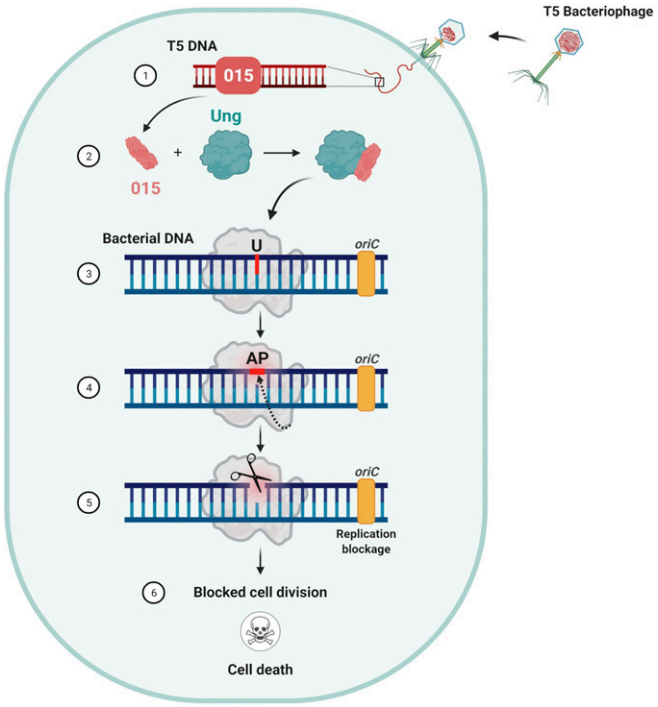

Fig. 7. Model of 015-mediated toxicity. T5 bacteriophage translocates its genetic material into the *E. coli* cell, which expresses 015 within several minutes (1). The 015 gene product forms a complex with the host Ung (2) and thus localizes to newly formed AP sites (3). 015 then attacks the AP site (4) and forms a nick in the chromosomal DNA (5), which leads to DNA replication arrest and ultimately to cell death (6).

concentrate on efficient replication of the phage DNA. In addition, halting cell division enables better resource utilization from both daughters of a dividing cell (15).

The growth of several well-known phages is inhibited when their DNA contains dUMP only if Ung is expressed by the host cell. Both λ and P1 phages grown in bacteria lacking dUTPase and Ung (thus, containing high dUMP levels in their DNA) cannot propagate in bacteria encoding Ung but propagate efficiently on bacteria lacking Ung (16). T5 and T4 phages encode their own dUTPase for eliminating dUMP from their genome. Therefore, wild type T4 and T5 grown in bacteria lacking dUTPase and Ung propagate in bacteria expressing Ung, but mutant T4 and T5 lacking their dUTPase fail to propagate in bacteria expressing Ung (16, 17). These observations suggest that the mechanism reported here for cleavage of dUMP-containing DNA is general for many phage types, whereas the detailed mechanism of DNA cleavage may differ between these groups. The phylogenic distribution shown for homologs of the 015 protein further strengthens the widespread nature of this protein and suggests that many phages use it along with Ung for cleaving the host DNA.

Although we found that 015 can cleave AP sites in the absence of Ung in vitro, the presence of Ung is essential for the 015-mediated toxic activity in vivo. This apparent contradiction can be explained if one considers the difference in length of the target DNA molecules. The dsDNA oligomer used in our in vitro assay is short, and therefore 015 can locate the AP site on it, whereas binding to the Ung in the cell may be required for efficient localization to nascent AP sites on the long bacterial chromosome. Indeed, microscopy experiments clearly show colocalization of 015 and Ung. In addition, utilizing Ung to identify the AP sites may be advantageous from the phage's perspective since it ensures that 015 localizes to a newly made AP site before the cell has had a chance to repair the DNA damage by using the base-excision repair pathway.

We determined that the nick formed by 015 has similar mobility to that formed by Ape1, suggesting that the hydrolytic strand cleavage at the AP site produces a 5′-dRP. The absence of a base attached to the C1′ position in the 5′-dRP terminus renders it highly reactive. Therefore, the 5′-dRP may cross-link with exocyclic amine of the opposite DNA strand or with proteins, thus producing a DNA–DNA interstrand cross-link (ICL) or a DNA–protein cross-link (DPC), respectively (18–20). Although identical intermediates are formed during base-excision repair, they may be stabilized by the processing enzymes, while 015 may not stabilize these intermediates. Therefore, the cross-linking reactions, in turn, could block replication. We hypothesize that the frequent 015-induced nicks generate ICL or DPC that cause the observed DNA replication halt and consequent inhibition of cell growth.

The mechanism revealed in this study enhances our understanding of the molecular tools used by phages to manipulate and exploit host cells. The specific targeting of Ung-generated AP sites by 015 may be adapted to develop antibacterial treatments as well as to develop molecular biology tools that will facilitate specific cleavage of uracil-containing DNA. We predict that the approach described here can be harnessed to reveal additional mechanisms used by phage proteins to inhibit bacterial cells, which may lead to the discovery of new targets for antibacterial drug design.

Experimental Procedures

Strains, media, reagents, and plasmids are described in the *SI Appendix*.

Phylogenetic distribution of 015 homologs, growth inhibition assay, the isolation of resistant mutants and high-throughput sequencing, the generation of nontoxic 015 mutant using site-directed mutagenesis, the purification of His-maltose-binding protein (MBP)–tagged Ung and His-tagged H-NS, and the in vitro pull-down assay are also described in the *SI Appendix*.

Pull-Down Assay. *E. coli* BW25113 Δ*ung* strain was cotransformed with the isopropyl β- d-1-thiogalactopyranoside (IPTG)-inducible pUng and the arabinose-inducible plasmid pBAD18-015 containing a CBP tag (pBAD18:015-CTAP), its mutant form (pBAD18:015$^{K85A\ K94A\ K111A}$-CTAP), or a plasmid for expression of CBP-tagged phage T7 protein 1.4 (pBAD18:1.4-CTAP), which was used as control. Transformants were grown overnight in LB supplemented with ampicillin, chloramphenicol, and 0.2% (wt/vol) D-glucose at 37 °C, and then cultures were diluted 1:100 in fresh 10 mL LB supplemented with ampicillin and chloramphenicol; cultures were grown at 37 °C until reaching optical density $(OD)_{600} = 0.5$, when expression of indicated proteins was induced by adding 0.2% (wt/vol) L-arabinose and 1 mM IPTG. Cultures were grown for another 2 h and then harvested by centrifugation at 4,000 × *g* for 10 min and resuspended in 500 μL BugBuster reagent (Merck) supplemented with 200 μg/mL lysozyme (Sigma) and 1× protease inhibitor mixture (Sigma). Cell suspensions were then incubated at room temperature (RT) for 20 min on a rotating mixer. Cell debris was cleared by centrifugation for 30 min at 16,000 × *g* at 4 °C, and supernatant (70 μL) was used as the input fraction. The remaining supernatant was mixed with 70 μL nickel-nitrilotriacetic acid (Ni-NTA) resin (Invitrogen) and incubated on a rotating mixer for 30 min at 4 °C. The resin was then washed with 5 mL of wash buffer A (50 mM Na-phosphate buffer pH 7.6, 500 mM NaCl, and 40 mM Imidazole) followed by wash buffer B (50 mM Na-phosphate buffer pH 7.6, 1 M NaCl, and 40 mM Imidazole) and wash buffer C (50 mM Na-phosphate buffer pH 7.6, 1.5 M NaCl, and 40 mM Imidazole). Bound proteins were eluted with 90 μL of elution buffer (50 mM Na-phosphate buffer pH 7.6, 500 mM NaCl, and 300 mM Imidazole). The output eluted fractions and the input fractions were mixed with 4× protein loading dye (Bio-Rad) and boiled for 10 min at 95 °C. The samples were resolved on a 4 to 20% TGX stain free gel (Bio-Rad), transferred to a 0.2-μm nitrocellulose membrane, and immunoblotted with anti-CBP antibodies (diluted 1:1,000; Merck #07-482) to detect 015-CBP or 1.4-CBP and with anti-His antibody (diluted 1:250) to detect the expression of Ung-His.

Expression and Purification of His-Tagged 015. *E. coli* BL21-AI Δ*ung* strain was generated by P1 transduction, as described previously (21), using *E. coli* BW25113 Δ*ung*::kan as the donor strain, followed by flipping out the kanamycin cassette using plasmid PCP20 (22). BL21-A1 Δ*ung* was then transformed with the arabinose-inducible pBAD:015-Myc-His plasmid. A transformed colony was grown overnight in LB supplemented with kanamycin at 37 °C. In the morning, the culture was diluted 1:100 into 4 L of fresh LB supplemented with

kanamycin and incubated at 37 °C until it reached an $OD_{600} = 0.5$. L-Arabinose (0.2% wt/vol) was then added to induce 015 expression, and the culture was incubated for 4 additional hours at 37 °C. Cells were then harvested by centrifugation at 4,000 × *g* for 20 min and resuspended in 60 mL of Lysis buffer (20 mM Tris-Cl pH 8.0, 500 mM NaCl, 10 mM Imidazole, 5% vol/vol Glycerol, and 1 mM phenylmethylsulfonyl fluoride [PMSF]). The cell suspension was lysed by sonication on ice, and cell debris was removed by centrifugation for 1 h at 16,000 × *g* at 4 °C. The cleared supernatant fraction was mixed with 500 μL of Ni-NTA Agarose resin (Invitrogen) and loaded onto an empty column. The 015-His bound resin was washed with 10 mL of wash buffer A (20 mM Tris-Cl pH 8.0, 500 mM NaCl, 40 mM Imidazole, and 5 mM β-mercaptoethanol), followed by 10 mL of wash buffer B (20 mM Tris-Cl pH 8.0, 1 M NaCl, 40 mM Imidazole, and 5 mM β-mercaptoethanol) and 1 mL of wash buffer C (20 mM Tris-Cl pH 8.0, 1 M NaCl, and 80 mM Imidazole). The bound 015-His protein was eluted from the column with 3 mL of elution buffer (20 mM Tris-Cl pH 8.0, 500 mM NaCl, and 300 mM Imidazole) and dialyzed against dialysis buffer (20 mM Tris-Cl pH 8.0 and 500 mM NaCl). The dialyzed 015-His was concentrated on Amicon Ultra-4 Centrifugal Filter Units (3 kDa columns) and loaded onto a Superdex 200 Increase 10/300 size exclusion chromatography column (GE Healthcare) equilibrated with a protein buffer (20 mM Tris pH 8.0 and 500 mM NaCl). Elution fractions (500 μL) were collected, and the fractions corresponding to 17 to 20 mL of eluate were pooled and dialyzed against a final dialysis buffer (20 mM Tris-Cl pH 8.0 and 150 mM NaCl). The purified protein was then concentrated on Amicon Ultra-4 Centrifugal Filter Units (3 kDa columns) and resolved on a sodium dodecyl sulphate-polyacrylamide gel electrophoresis (SDS-PAGE) followed by Coomassie brilliant blue staining of the gel to confirm purity. Purified protein was flash-frozen in liquid N_2 and stored at −80 °C for subsequent use.

Fluorescence Microscopy. To study the localization of Ung and 015 using fluorescence microscopy, *E. coli* BW25113 Δ*ung* cells containing arabinose-inducible pBAD18:015-sfGFP (p015-sfGFP) or pBAD18:015$^{K85A\ K94A\ K111A}$-sfGFP (p015$^{K85A\ K94A\ K111A}$-sfGFP) and pBAD33.1^{Strp} (V) or pBAD33.1^{Strp}:Ung-mCherry (pUng-mCherry) plasmids were grown overnight at 37 °C in LB supplemented with ampicillin, streptomycin, and 0.2% (wt/vol) D-glucose. Cultures were diluted 1:100 in 3 mL of fresh LB supplemented with ampicillin, streptomycin, and 0.2% (wt/vol) D-glucose and incubated at 37 °C until they reached an OD_{600} = 0.3. Cells were then washed twice with fresh LB to remove the glucose and were resuspended in 3 mL LB supplemented with ampicillin, streptomycin, and 0.01% (wt/vol) L-arabinose to induce expression from pBAD plasmids. Cultures were incubated for 30 min under the same conditions, and the cells were then harvested by centrifugation at 4,000 × *g* for 10 min, washed twice with M9 media, and stained for 10 min at RT with Hoechst 33342 at a final concentration of 1 μg/mL. The cells were then washed twice and resuspended in 10 μL of M9 media. An aliquot of each cell suspension (2 μL) was spotted onto 1% (wt/vol) agarose pads, which were placed face-down in 35-mm glass-bottom Cellview cell culture dishes. Bacterial cells were imaged by a Nikon Eclipse Ti2-E inverted motorized microscope equipped with a CFI Plan apochromat DM 100× oil lambda PH-3 (NA, 1.45) objective lens, Lumencor SOLA SE II 395 light source, and DS-QI2 mono cooled digital microscope camera (16 MP). An ET-DAPI filter set (#4908) was used to visualize Hoechst 33342 signals, an ET-EGFP filter set (#49002) was used to visualize superfolder GFP (sfGFP) signals, and an RFP filter set (#49005) was used to visualize mCherry signals. The captured images were processed further using Fiji ImageJ suite (23).

To monitor the morphological changes in cells expressing 015, *E. coli* MG1655 cells harboring pBAD33^{Kan}-015 (p015^{Kan}) or empty pBAD33^{Kan} (V) plasmids were incubated overnight at 37 °C in LB supplemented with 50 μg/mL kanamycin and 0.2% (wt/vol) D-glucose. Cultures were then diluted 1:50 into fresh LB supplemented with kanamycin and 0.2% (wt/vol) D-glucose and incubated at 37 °C until they reached an $OD_{600} = 0.5$. The cells were washed twice with fresh LB to remove the glucose and then resuspended in 3 mL LB supplemented with kanamycin and 0.2% (wt/vol) L-arabinose to induce 015 expression. At the indicated time points, cells were harvested, stained with Hoechst 33342, and visualized under the microscope as described above.

Cleavage of dsDNA Oligomers. To generate a dsDNA oligomer containing an Ung-recognition site that can be detected by fluorescence, the following oligonucleotides were synthesized by Integrated DNA Technologies (IDT):

A) 5′ Cy5.5-CAATGATGTTACA/deoxyU/ATGAGATGGTCAGA 3′
B) 5′ TCTGACCATCTCATCTGTAACATCATTG 3′
C) 5′ CAATGATGTTACA/deoxyU/ATGAGATGGTCAGA-Cy5.5 3′.

The Cy5.5 fluorophore-conjugated, uracil-containing oligo (A) was annealed with the corresponding complementary oligo (B) in annealing buffer (10 mM Tris-Cl pH 8.0, 50 mM NaCl, and 1 mM ethylenediaminetetraacetic acid [EDTA]) by heating a 1:1 mixture of the two oligos at 95 °C for 5 min followed by slowly cooling the reaction mixture at a rate of 1 °C/min. AP site generation and cleavage assay were conducted in a 10-μL reaction containing 60 nM of annealed oligos treated with the indicated amounts of Ung (NEB) and either purified 015 or Ape1 endonuclease (NEB) in a reaction buffer containing 100 mM KCl, 5 mM MgCl2, 10 mM Tris-Cl (pH 8.0), 0.01% (vol/vol) Nonidet P-40, and 0.1 mg/mL bovine serum albumin (BSA). Reaction mixtures were incubated for 1 h at 37 °C. Equal volumes of formamide loading dye (95% vol/vol formamide, 20 mM EDTA, and 0.025% wt/vol bromophenol blue) were mixed with the reaction mixtures and loaded onto 20% polyacrylamide gels containing 7.5 M urea. Electrophoresis was carried out at 200 V for 4 h in 0.5× tris/borate/EDTA (TBE) buffer. Cy5.5 fluorescence was detected using Sapphire biomolecular imager (Azure biosystems).

To test the effect of 015 on Ung-pretreated DNA, Cy5.5 fluorophore-conjugated, uracil-containing annealed dsDNA oligos were treated with 33.4 nM Ung (NEB) for 1 h at 37 °C. Treated and untreated DNA was then purified using an equal volume of phenol–chloroform–isoamyl alcohol and incubation for 15 min at RT. Following centrifugation at 13,000 × *g* for 10 min, the aqueous solution was transferred into a new tube, and 1/10 volume of 3 M sodium acetate (pH 5.2) and 3 volumes of ice-cold absolute ethanol were added. The mixture was then incubated for 1 h at −80 °C followed by centrifugation at 13,000 × *g* for 30 min at 4 °C. The pellet was washed with 80% ethanol, allowed to dry, and then dissolved in 15 μL nuclease-free water (Qiagen). The purified Ung-treated DNA was treated with indicated concentrations of either purified 015 or Ape1 endonuclease (NEB) in a reaction buffer containing 100 mM KCl, 5 mM MgCl2, 10 mM Tris-Cl (pH 8.0), 0.01% (vol/vol) Nonidet P-40, and 0.1 mg/mL BSA.

To compare the ends of 015-cleaved products with products of known enzymes, 60 nM of cy5.5 conjugated annealed oligos were treated with 33.4 nM of Ung and 946 nM of 015, 33 nM of Ape1, 1.28 μM of Fpg, or 89.1 nM of Endonuclease III for 4 h at 37 °C. The cleaved products with 3′ termini end products were then separated by electrophoresis in 20% (wt/vol) polyacrylamide gel containing 7.5 M urea. The cleaved products with 5′ termini end products were stabilized with 100 mM $NaCNBH_3$ and then separated by electrophoresis in 25% (wt/vol) polyacrylamide gel containing 7 M urea.

For time-dependent experiments, 60 nM Cy5.5-conjugated, uracil-containing oligos were mixed with different concentration of 015 (283 nM, 567 nM, and 851 nM) and 33.4 nM of Ung in a reaction buffer containing 100 mM KCl, 5 mM MgCl2, 10 mM Tris-Cl (pH 8.0), 0.01% (vol/vol) Nonidet P-40, and 0.1 mg/mL BSA. The 50 μL of reaction mixtures were incubated at 37 °C, and 5 μL of mixture was taken out into a stopping buffer (20 mM EDTA, 1% SDS, and 190 μg/mL proteinase K) at different time points (0, 10, 20, 30, 60, 120, 240, and 360 min).

Determining the *oriC*/*ter* Ratio. *E. coli* MG1655 were transformed with pBAD33^{Kan}-015 (p015^{Kan}) or pBAD33 (V) plasmids. Transformants were grown overnight at 37 °C in LB supplemented with kanamycin and 0.2% (wt/vol) D-glucose. Cultures were diluted 1:100 in 10 mL fresh LB supplemented with kanamycin and 0.2% (wt/vol) D-glucose and grown at 37 °C until they reached $OD_{600} = 0.5$. Cells were then washed twice with fresh LB, resuspended in LB supplemented with kanamycin and 0.2% (wt/vol) L-arabinose to induce expression from the plasmids, and incubated at 37 °C for 2 additional hours. As a positive control, cells containing an empty plasmid (V) were treated at OD_{600} ~0.5 with 0.5 μg/mL of the DNA synthesis inhibitor, trimethoprim. For the reference control, in which the *oriC*/*ter* ratio is expected to be 1, the cells harboring pBAD33 (V) were treated with 150 μg/mL rifampicin at $OD_{600} = 0.3$ (24). Cells treated with rifampicin were incubated for 4 additional hours, and then 1 OD_{600} units were harvested and genomic DNA was isolated (Macherey-Nagel NucleoSpin Tissue kit). Isolated DNA (9 ng) was used as a template in a 10-μL real-time PCR mixture including 0.6 pmol forward and reverse primers (*SI Appendix*, Table S4) and 5 μL SYBR-green master mix (Applied Biosystem). Real-time PCR was conducted in a StepOne Real-Time PCR System using the following amplification protocols: 95 °C for 3 min followed by 40 cycles of 95 °C for 30 s, 60 °C for 30 s, and 72 °C for 30 s. The *oriC*/*ter* ratio was determined as previously described (24), using the following equation:

$$OriC \Big/ ter = \frac{{E_0}^{CT_{C,O} - CT_{S,O}}}{{E_t}^{CT_{C,t} - CT_{S,t}}},$$

where E_0 is the fold change per cycle for *oriC*, and E_t is the fold change per cycle for the terminus. $CT_{C,0}$ and $CT_{S,0}$ are the CT values of *oriC* for control or sample, respectively, and $CT_{C,t}$ and $CT_{S,t}$ are the CT values of terminus for control or sample, respectively.

Genome Coverage Analysis. Overnight cultures of *E. coli* MG1655 harboring pBAD33^{Kan}-015 (p015^{Kan}) or an empty pBAD33^{Kan} plasmid (V) were diluted 1:100 in fresh LB supplemented with kanamycin and 0.2% (wt/vol) D-glucose

MICROBIOLOGY

and grown at 37 °C. When the cultures reached OD_{600} = 0.05, L-arabinose was added (0.2% wt/vol) to induce 015 expression, and the cultures were incubated for 2 additional hours at 37 °C. After this time, 1 OD_{600} units were harvested and total DNA was isolated (Macherey-Nagel NucleoSpin Tissue kit). The concentration and purity of the isolated DNA were evaluated using a NanoDrop 2000 spectrophotometer. The experiments were conducted in biological triplicates.

To perform the DNA-seq, 1 μg genomic DNA was mechanically sheared using Covaris E220X to yield fragments ~300 bp. Sheared DNA was run on TapeStation (Agilent) to ensure accurate shearing. Libraries were prepared from 300 to 1,000 ng of DNA as previously described (25). Libraries were quantified by Qubit (Thermo Fisher Scientific) and TapeStation (Agilent). Sequencing was done on a MiSeq instrument (Illumina) using a V2 300 cycle kit, allocating ~2 M reads per sample (paired-end sequencing).

For variant calling, Illumina adapters were trimmed from the reads using cutadapt (26); resulting reads shorter than 30 bp were discarded. Reads were mapped using bwa (bwa-0.7.5a) to the *E. coli* MG1655 Ensembl GCA_000005845.2 genome. Mapped reads were further processed with GATK v.3.7. Variants were called using the GATK HaplotypeCaller with ploidy set to 10. Variants were filtered with the following values for SNPs and Indels, respectively: QD < 2.0, FS > 60.0, MQ < 40.0, MQRankSum < −12.5, ReadPosRankSum < −8.0, HaplotypeScore > 13.0, and QD < 2.0, FS > 200.0, and ReadPosRankSum < −20.0. Ensembl's Variant Effect Predictor was used for annotation (https://bacteria.ensembl.org/index.html).

To determine the depth of coverage, reads were mapped using bwa (bwa-0.7.5a) to the *E. coli* MG1655 Ensembl GCA_000005845.2 genome. Reads were then deduplicated using Picard. To calculate per base coverage, we used GATK v.3.7 "Depth of Coverage." Igvtools was used (IGV Version 2.3.25) for a coverage window of 1,000 bp. Counts for each sample were scaled (*z*-score) by subtracting the mean and dividing by the SD.

Data Availability. All study data are included in the article and/or *SI Appendix*.

ACKNOWLEDGMENTS. U.Q. and D.S. have received funding from the European Research Council under the European Union's Horizon 2020 research and innovation program (Grant Nos. 818878 and 714224, respectively). U.Q. has received funding from the Israeli Ministry of Science (Grant No. 3-14351) and the Israeli Ministry of Health in the framework of the ERANET-JPI-AMR (Grant No. 15370). O.A. was supported in part by a fellowship from the Edmond J. Safra Center for Bioinformatics at Tel Aviv University by the Dalia and Eli Hurvitz Foundation. We thank Dr. Dayana Yahalomi from The Mantoux Bioinformatics and the Crown Genomics institutes, Weizmann Institute of Science, for sequencing and analyses.

1. R. Kiro *et al*., Gene product 0.4 increases bacteriophage T7 competitiveness by inhibiting host cell division. *Proc. Natl. Acad. Sci. U.S.A.* **110**, 19549–19554 (2013).
2. S. Molshanski-Mor *et al*., Revealing bacterial targets of growth inhibitors encoded by bacteriophage T7. *Proc. Natl. Acad. Sci. U.S.A.* **111**, 18715–18720 (2014).
3. J. Davison, Pre-early functions of bacteriophage T5 and its relatives. *Bacteriophage* **5**, e1086500 (2015).
4. T. Lindahl, An N-glycosidase from Escherichia coli that releases free uracil from DNA containing deaminated cytosine residues. *Proc. Natl. Acad. Sci. U.S.A.* **71**, 3649–3653 (1974).
5. T. Lindahl, S. Ljungquist, W. Siegert, B. Nyberg, B. Sperens, DNA N-glycosidases: Properties of uracil-DNA glycosidase from Escherichia coli. *J. Biol. Chem.* **252**, 3286–3294 (1977).
6. T. Lindahl, Repair of intrinsic DNA lesions. *Mutat. Res.* **238**, 305–311 (1990).
7. L. M. Guzman, D. Belin, M. J. Carson, J. Beckwith, Tight regulation, modulation, and high-level expression by vectors containing the arabinose PBAD promoter. *J. Bacteriol.* **177**, 4121–4130 (1995).
8. T. Baba *et al*., Construction of Escherichia coli K-12 in-frame, single-gene knockout mutants: The Keio collection. *Mol. Syst. Biol.* **2**, 2006.0008 (2006).
9. Q. Chai *et al*., Organization of ribosomes and nucleoids in Escherichia coli cells during growth and in quiescence. *J. Biol. Chem.* **289**, 11342–11352 (2014).
10. X. Giroux, W. L. Su, M. F. Bredeche, I. Matic, Maladaptive DNA repair is the ultimate contributor to the death of trimethoprim-treated cells under aerobic and anaerobic conditions. *Proc. Natl. Acad. Sci. U.S.A.* **114**, 11512–11517 (2017).
11. E. J. Diner, C. M. Beck, J. S. Webb, D. A. Low, C. S. Hayes, Identification of a target cell permissive factor required for contact-dependent growth inhibition (CDI). *Genes Dev.* **26**, 515–525 (2012).
12. P. M. Johnson *et al*., Unraveling the essential role of CysK in CDI toxin activation. *Proc. Natl. Acad. Sci. U.S.A.* **113**, 9792–9797 (2016).
13. A. M. Jones, F. Garza-Sánchez, J. So, C. S. Hayes, D. A. Low, Activation of contact-dependent antibacterial tRNase toxins by translation elongation factors. *Proc. Natl. Acad. Sci. U.S.A.* **114**, E1951–E1957 (2017).
14. H. R. Warner, L. K. Johnson, D. P. Snustad, Early events after infection of Escherichia coli by bacteriophage T5. III. Inhibition of uracil-DNA glycosylase activity. *J. Virol.* **33**, 535–538 (1980).
15. R. Kiro, D. Shitrit, U. Qimron, Efficient engineering of a bacteriophage genome using the type I-E CRISPR-Cas system. *RNA Biol.* **11**, 42–44 (2014).
16. H. R. Warner, R. B. Thompson, T. J. Mozer, B. K. Duncan, The properties of a bacteriophage T5 mutant unable to induce deoxyuridine 5′-triphosphate nucleotidohydrolase. Synthesis of uracil-containing T5 deoxyribonucleic acid. *J. Biol. Chem.* **254**, 7534–7539 (1979).
17. H. R. Warner, B. K. Duncan, In vivo synthesis and properties of uracil-containing DNA. *Nature* **272**, 32–34 (1978).
18. R. W. Sobol *et al*., The lyase activity of the DNA repair protein beta-polymerase protects from DNA-damage-induced cytotoxicity. *Nature* **405**, 807–810 (2000).
19. S. J. Admiraal, P. J. O'Brien, Reactivity and cross-linking of 5′-terminal abasic sites within DNA. *Chem. Res. Toxicol.* **30**, 1317–1326 (2017).
20. R. W. Sobol *et al*., Base excision repair intermediates induce p53-independent cytotoxic and genotoxic responses. *J. Biol. Chem.* **278**, 39951–39959 (2003).
21. I. Yosef, M. G. Goren, R. Kiro, R. Edgar, U. Qimron, High-temperature protein G is essential for activity of the Escherichia coli clustered regularly interspaced short palindromic repeats (CRISPR)/Cas system. *Proc. Natl. Acad. Sci. U.S.A.* **108**, 20136–20141 (2011).
22. K. A. Datsenko, B. L. Wanner, One-step inactivation of chromosomal genes in Escherichia coli K-12 using PCR products. *Proc. Natl. Acad. Sci. U.S.A.* **97**, 6640–6645 (2000).
23. J. Schindelin *et al*., Fiji: An open-source platform for biological-image analysis. *Nat. Methods* **9**, 676–682 (2012).
24. J. Slager, M. Kjos, L. Attaiech, J. W. Veening, Antibiotic-induced replication stress triggers bacterial competence by increasing gene dosage near the origin. *Cell* **157**, 395–406 (2014).
25. R. Blecher-Gonen *et al*., High-throughput chromatin immunoprecipitation for genome-wide mapping of in vivo protein-DNA interactions and epigenomic states. *Nat. Protoc.* **8**, 539–554 (2013).
26. M. Martin, Cutadapt removes adapter sequences from high-throughput sequencing reads. *EMBnet. J.* **17**, 10–12 (2011).